

HIGH INTENSITY ASPECTS OF J-PARC LINAC INCLUDING RE-COMMISSIONING AFTER EARTHQUAKE

M. Ikegami, K. Futatsukawa, T. Miyao, Y. Liu, KEK/J-PARC, Tokai, Japan
T. Maruta, A. Miura, J. Tamura, JAEA/J-PARC, Tokai, Japan

Abstract

In the course of the beam commissioning of J-PARC linac after nine-month shutdown due to an earthquake, we have experienced beam losses which were not seen before the earthquake. One of the main cause for the beam loss was the irregular RF setting for accelerating cavities to avoid multipactor at a cavity, which started to pose difficulty in the nominal operation after the earthquake. In an effort to mitigate the beam loss, we tried a few RF settings, some of which resulted in noticeable beam loss. In this paper, we discuss the particle simulation attempted to reproduce the beam loss with the irregular RF setting, and its comparison with the experimental result.

INTRODUCTION

We had a magnitude-9.0 earthquake in Tohoku region in Eastern Japan in March 2011. It caused severe damage to J-PARC facilities which forced us to shutdown for nearly nine months [1]. After significant restoration efforts, we started beam operation of J-PARC linac in December 2011 and user operation in January 2012. The linac beam power when we resumed the user operation was 7.2 kW. Then, it is increased to 13.3 kW in March 2012, which is the same as just before the earthquake. While the linac beam operation was restored in terms of the beam power, we have experienced higher beam losses than before the earthquake. Thus, we have been trying to mitigate the beam loss while supporting the user operation.

One of the main causes of the beam loss was multipactor at an accelerating cavity, which started to pose difficulty in the nominal operation after the earthquake. The multipactor forced us to adopt irregular RF setting, which resulted in excess beam losses. After trying a few RF settings, we finally succeeded in suppressing the beam loss to a comparable level to before the earthquake.

The history of the beam start-up after the earthquake was reported in other literatures [2, 3, 4]. Then, we don't reiterate it in this paper. Instead, we discuss in this paper a particle simulation study intended to reproduce the beam loss we experienced in the beam commissioning.

This paper is organized as follows. We start with briefly reviewing the multipactor at an accelerating cavity in the next section. Then, we describe three RF settings we tried to avoid the multipactor in the beam commissioning. After presenting the experimentally observed beam losses, we move to particle simulation. We then try to deduce a picture on the mechanism for the experimentally observed beam loss comparing the experimental and simulation results.

MULTIPACTOR AT AN RF CAVITY

J-PARC linac consists of a 50-keV negative hydrogen ion source, 3-MeV RFQ (Radio Frequency Quadrupole linac), 50-MeV DTL (Drift Tube Linac), and 181-MeV SDDL (Separate-type DTL) [5]. The multipactor mentioned above is observed in one of SDDL tanks. The SDDL section consists of 30 SDDL tanks with $2\beta\lambda$ inter-tank spacing. Here, β and λ denote the particle velocity scaled by the speed of light and the RF wavelength, respectively. Each SDDL tank consists of five β -graded cells, and two neighboring SDDL tanks are driven by a klystron. The relative RF amplitude and phase of the tank pair are supposed to be kept balanced with the low-level RF control system. However, we noticed just before the resumption of beam operation in December 2011 that the fifth tank pair, or SDDL5, shows some unstable behavior. For this tank pair, one of the tanks tends to have arcing, or presumably multipactor, which makes the balance of RF amplitude and phase easily lost. This unstable behavior arises in a certain range of RF amplitude which contains its design amplitude. Although similar behavior has been noticed for SDDL1 to SDDL6 since before the earthquake, it caused no difficulty in operating with the design tank level [6]. Therefore, we suspect that the multipactor in SDDL5 become severer at the earthquake for some reason to cause practical difficulty in the nominal operation.

As we can avoid the multipactor by adopting higher or lower RF amplitude for SDDL5, we adopt 109 % of the design amplitude in starting the user operation in January 2012. However, the unstable band was widened during the beam operation and forced us to increase the operating amplitude to 116 % later. In this paper, we focus on the operation with 116 % amplitude for SDDL5. We don't delve into the details on the multipactor itself. Further detail of the multipactor will be found in the reference [7].

THREE RF SETTINGS

We here describe three RF settings we tried to avoid multipactor at SDDL5. We assume the RF amplitude of 116 % for SDDL5 in these cases.

Case-I: Phase-amplitude Scan Tuning Result

In setting the RF amplitude and phase for SDDL tanks after the earthquake, it was required for us to perform the phase and amplitude scan tuning [8]. In the tuning, we needed an unusual treatment for SDDL5. Namely, we fixed the amplitude for SDDL5 to be 116 % of the design and performed the phase scan only to find the phase setting to realize the design energy gain. After conducting the tuning

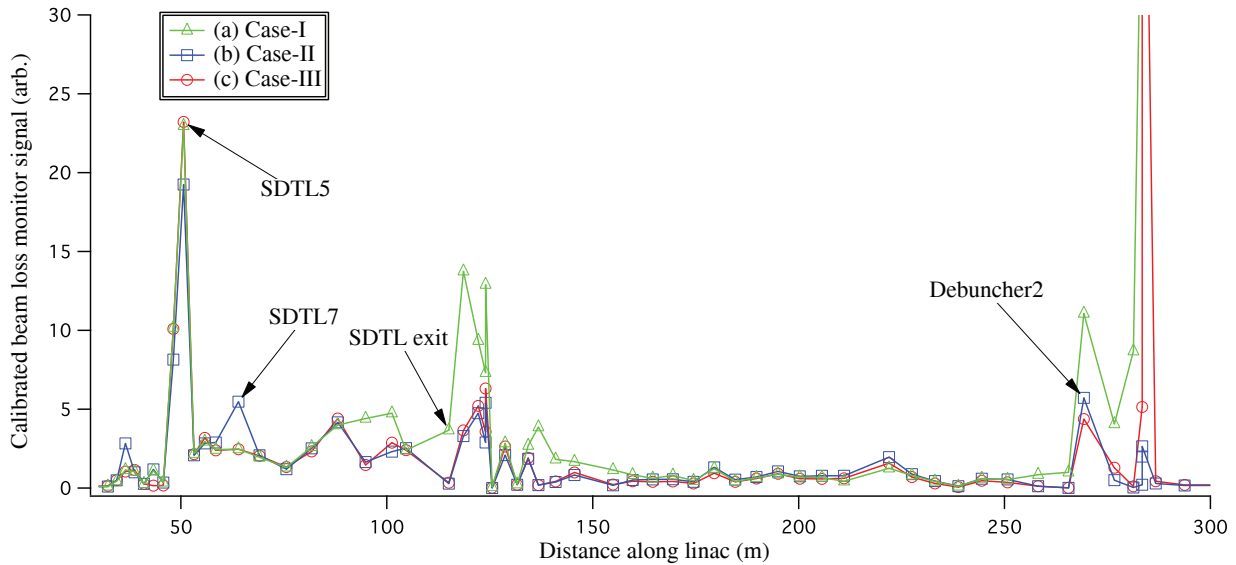


Figure 1: Calibrated beam loss monitor signal distribution along J-PARC linac and the following straight line of the beam transport line. Each marker shows the measured data with a beam loss monitor. The data are taken with the RF setting of (a) Case-I, (b) Case-II, and (c) Case-III.

for SDTL5, the tuning for SDTL6 and downer stream tanks were performed with the nominal procedure to set them to the design amplitude and synchronous phase. We denote the RF setting we find with this tuning as “Case-I”.

Case-II: Phase-shift Tuning Result

After finishing the phase and amplitude scan tuning, we tried to operate with the determined RF setting. However, we experienced significant beam loss as discussed later. We then tried to mitigate the beam loss by adjusting only the SDTL phases, because neighboring tanks also has multipactor bands in their amplitude and the varying the amplitude involves a risk to hit them. In this tuning, we adopt the phase shift for SDTL5 and that for SDTL6 to SDTL15 as two tuning knobs. It should be noted here that we assume the same phase shift for SDTL6 to SDTL15. This tuning was performed with the trial-and-error method to minimize the beam loss downstream with Case-I setting as the starting point. As a result, the phase for SDTL5 was shifted by -6 degree and those for SDTL6 to SDTL15 by +8 degree. Here, the positive phase shift is defined to increase the energy gain in the vicinity of the design phase. We call this RF setting “Case-II” in this paper.

Case-III: Design Longitudinal Focusing

In the last RF setting, we intend to adopt an optics with the design longitudinal focusing strength. Keeping the design longitudinal focusing with increased RF amplitude, we naturally have higher energy gain. Consequently, we need to reduce the energy gain for neighboring cavities to compensate it. As mentioned above, we have multipactor for SDTL1 to SDTL6, which poses a constraint in choosing their RF amplitude. We conducted detailed RF

measurements to confirm that we can decrease the SDTL4 amplitude while avoiding the multipactor. Then, we tried an RF setting where we keep the longitudinal focusing for SDTL5 to the design strength with 116 % amplitude. Its excess energy gain is compensated by lowering SDTL4 amplitude. In this setting, the longitudinal focusing for SDTL4 is also kept to the design strength. We here call this setting “Case-III”. In calculating the longitudinal focusing force, we adopt the single gap approximation for SDTL4 and SDTL5 neglecting the phase slip. In the setting, the energy gain of SDTL5 is increased from the design value of 8.35 MeV to 10.00 MeV. Meanwhile, the energy gain of SDTL4 is decrease from its design 7.55 MeV to 5.90 MeV with the reduced amplitude of 83 %.

EXPERIMENTAL OBSERVATION

Figure 1 shows the experimentally observed beam loss during the beam commissioning, where the beam loss is measured with BLM’s (Beam Loss Monitors) of gas proportional counter type [9] distributed along the linac. As the output from BLM tends to saturate, we perform a calibration to linearize it [10]. The calibrated BLM signal with the RF setting of Case-I is shown in Fig. 1 as (a). In the SDTL section with the horizontal axis of 30 to 115 m, the BLM is affected by X rays from SDTL cavity. A large peak is noticed around 50 m, which is supposedly caused by X rays from SDTL5 operating with higher RF amplitude than usual. Then, it is not caused by beam loss. It is readily seen in this figure that there is significant beam loss around the SDTL exit. We didn’t conduct a long-term operation with this setting due to the severe beam loss. As this data is taken while injecting the beam to the straight beam dump, the BLM’s after 250 m are affected by the reflection from

the beam dump.

The beam loss observed with the RF setting of Case-II is shown in Fig. 1 as (b). While the beam loss at around the SDTL exit is reasonably suppressed in this case, that in the middle of the SDTL section (around SDTL7) arises instead. Assuming the beam loss with lower energy would be preferable as the resultant residual radiation could be lower, we conducted a certain period of user operation with this setting. After 10 days of 7.2 kW operation and 8 days of 13.3 kW operation, we found however the residual radiation around SDTL7 reached 4 mSv/h on contact to the vacuum chamber several-hour after beam shutdown. As the high radiation dose is found in the neighboring two inter-tank spaces, the beam loss is supposedly distributed to a few to several meters longitudinally.

The beam loss observed with the RF setting of Case-III is shown in Fig. 1 as (c). The beam loss in the middle of SDTL section has been mitigated with this setting, while suppressing the beam loss around the SDTL exit. After adopting this RF setting, the residual radiation dose around SDTL7 started to decay while operating with 13.3 kW. Then, the residual radiation dose along the linac is decreased to a comparable level before the earthquake. The data shown as (b) and (c) in Fig. 1 are not affected by the reflection from the straight beam dump. Then, the sharp increase of the beam loss around 270 m in Case-II reflects a beam loss at the first bending magnet in the first arc section. The cause of this beam loss was identified later as the proton component accelerated by RFQ and mitigated by adjusting the chicane between RFQ and DTL [10].

PARTICLE SIMULATION

It is not usual to operate a β -graded linac with irregular RF settings for a long term. The experimental result described in the previous section then could provide us with a rare opportunity of code benchmarking on its ability of reproducing the beam loss. We here intend to reproduce the residual radiation level of several mSv/h on contact several-hour after beam shutdown of a few weeks of around 10 kW beam.

Simulation Condition

In the particle simulation, we adopt a three-dimensional PIC (Particle-In-Cell) code IMPACT [11]. Then, we employed 953,220 macro particles and $32 \times 32 \times 64$ meshes. We adopt the Lorentz integrator with the integration step width of around $\beta\lambda/100$. The simulation is conducted from the exit of RFQ to the middle of straight section after the SDTL exit assuming the same peak current of 15 mA as the experiment. The initial particle distribution of 95,322 particles is generated with PARMTEQ [12, 13], and then it is increased ten-fold by introducing small random variations for its coordinates.

Further, we assume the following errors:

- RF phase error of ± 1 degree.
- RF amplitude error of ± 1 %.
- Quadrupole transverse alignment error of ± 0.1 mm.

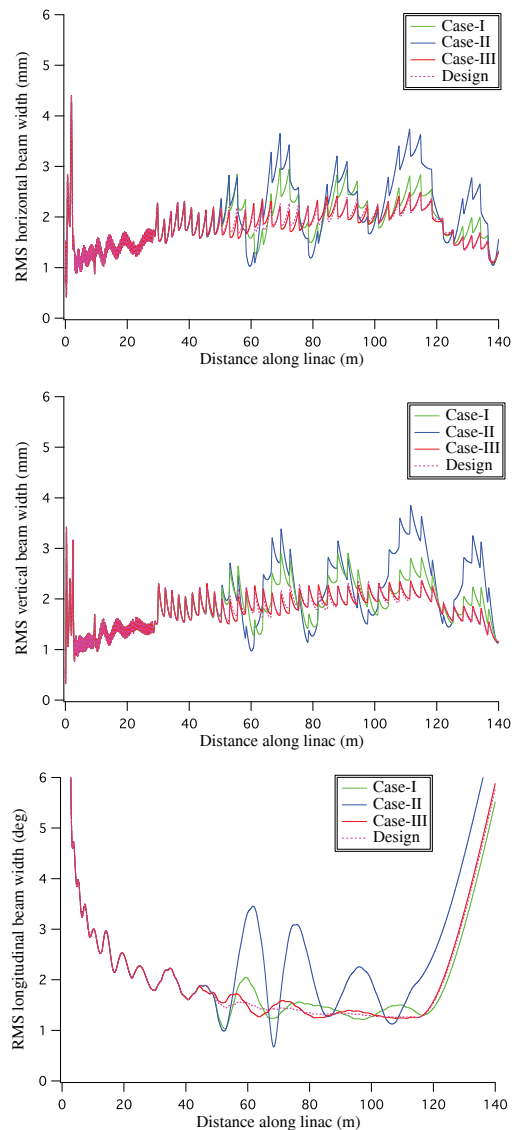


Figure 2: Simulated evolution of the rms beam envelope in the horizontal (top), vertical (middle) and longitudinal (bottom) directions. No random error is assumed. The envelope in Case-I, Case-II, and Case-III are shown with green, blue, and red solid lines, respectively. The result with the design RF setting is also shown with magenta broken lines.

- Quadrupole gradient error of ± 1 %.

We generate the errors with a uniform random generator within the ranges specified above. Then, 20 different random seeds are employed for each case.

Simulation Result

We first conduct a simulation without a random error, and see the evolution of root-mean-squared (rms) beam envelopes in the three cases mentioned in the previous section. Figure 2 shows the simulated beam envelopes. It is readily seen in this figure that the most severe longitudinal mismatch is induced in Case-II, and the transverse oscillation is also induced almost immediately. Comparing

the envelope evolution between Case-I and Case-II, we find it counter-intuitive that the experimentally observed beam loss appears to be lower in Case-II.

In the error simulation in Case-I, the beam loss is mostly localized in the first DTL tank, or DTL1, and the transition between DTL and SDTL. We observe a small loss around the SDTL exit only with one seed out of 20. The beam loss distribution with this seed is shown as the top figure in Fig. 3. In this figure, DTL1 locates from 3 to 12 m in the horizontal axis and the DTL-SDTL transition at 30 m.

Meanwhile, we find specifically localized beam loss around SDTL7 with 7 seeds out of 20 in Case-II. A typical beam loss distribution for those seeds is shown as the middle figure in Fig. 3. The loss location around SDTL7 agrees with the experiment. However, all the results with those seeds are accompanied by more significant beam loss around the SDTL exit, which is not consistent with the experimental observation. With other seeds, the beam loss is localized in DTL1 and the DTL-SDTL transition with occasional beam loss around the SDTL exit.

In Case-III, the beam loss is localized in DTL and the DTL-SDTL transition with all seeds. It involves the lowest beam loss in these three cases, which agrees with the experiment.

Then, the particle simulation reproduces the tendency to have localized beam loss around SDTL7 in Case-II. However, it does not reproduce the beam loss around the SDTL exit which is more significant in Case-I than in Case-II in the experiment.

DISCUSSION

To deepen our understanding on the beam loss observed in the simulation, we closely look into a result in Case-II which have a localized beam loss around SDTL7 (with the same random seed as the middle figure in Fig. 3). Figure 4 shows the simulated phase space beam distribution at the entrance of SDTL5. In this figure, the particles which survive through the linac are shown with red dots, those lost around SDTL7 with blue crosses, and those lost around the SDTL exit with green crosses. It is readily seen in this figure that the particles lost around SDTL7 locate at the transverse edge of the beam at the SDTL5 entrance. It indicates that the beam loss at SDTL7 is induced by a simple transverse scraping. Namely, the particles located at an edge of the beam are lost with too significant transverse oscillation. This type of beam loss tends to occur at SDTL7 with the perturbation applied at SDTL5. Meanwhile, it is seen in Fig. 4 that the particles lost around the SDTL exit locate next to those lost at SDTL7 but slightly nearer to the beam center. It indicates that the beam loss at SDTL7 and the SDTL exit are caused by the same mechanism. Then, the particles which narrowly survive at SDTL7 are finally lost at the SDTL exit due to increasing transverse oscillation amplitude. The particle simulation for Case-II provides us with this simple picture for the mechanism of the beam loss.

In the experiment, however, we have significant beam

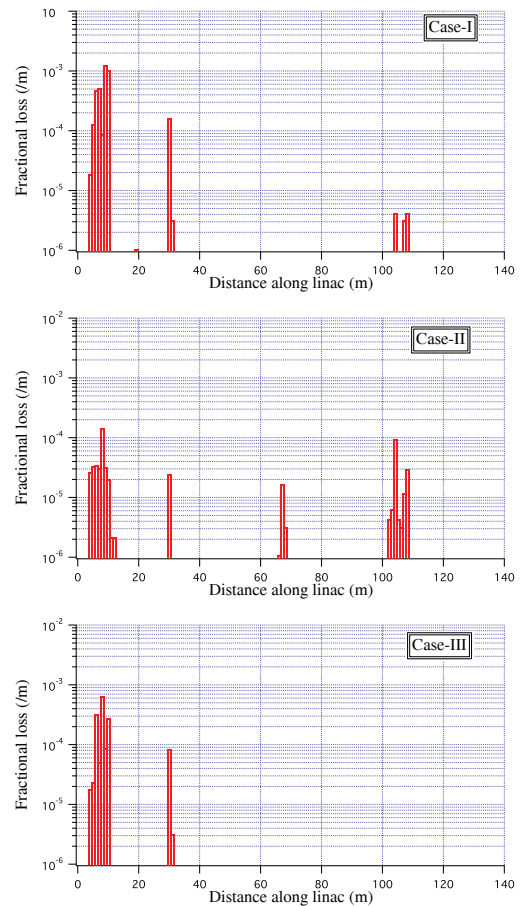


Figure 3: Simulated beam loss distribution along the linac. A characteristic result with a random seed is shown for each case. The top figure shows the only result with the beam loss around the SDTL exit in Case-I. The middle figure shows a typical result with the beam loss around SDTL7 in Case-II. The bottom figure is a typical result in Case-III.

loss at SDTL7 without that around the SDTL exit in Case-II. The picture provided by the simulation leads us to conclude that the beam loss could be caused by satellite particles. Namely, there are particles which are located far from the beam center and lost around SDTL7. However, there are no particles which are located just inside of those particles. The particle simulation indicates that they will be lost around the SDTL exit if they exist. It means that there is a gap in distribution between the particles lost around SDTL7 and those survive through the linac, which separates the satellite particles from the main bunch. The counter-intuitive beam loss behavior we experienced in the experiment can be explained by assuming satellite particles. We are currently looking into beam profile measurement data to see if there is a sign of satellite particles.

If the satellite particles consists of protons, it explains the sudden increase of the beam loss at the first bending magnet experimentally observed in Case-III. Protons can be generated in a double-stripping scattering with residual gas in a

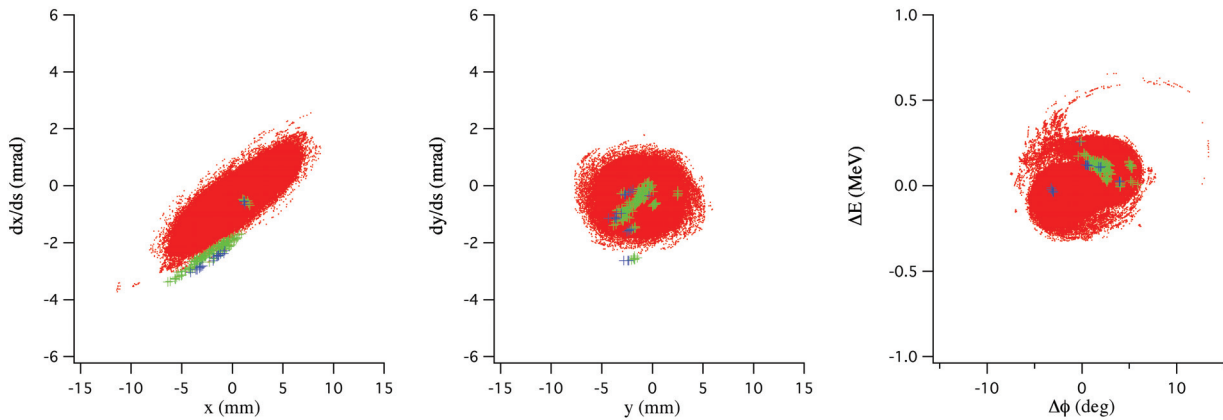


Figure 4: Simulated beam distribution for Case-II at the entrance of SDDL5 in the horizontal (left), vertical (middle), and longitudinal (right) phase planes. The particles which survive through are shown with red dots, those lost around SDDL7 with blue crosses, and those lost around the SDDL exit with green crosses.

beam transport line between the ion source and RFQ. Then, they can be captured by RFQ to the opposite RF phase to negative hydrogen ions and accelerated by the linac. We have experienced beam losses caused by such protons [10], and we have experimentally confirmed that the beam loss at the first bending magnet in Case-III is caused by this mechanism.

SUMMARY

We had a large earthquake in March 2011 followed by a nine-month beam shutdown for restoration efforts. In the course of the beam commissioning after the earthquake, multipactor at an SDDL cavity has forced us to operate with irregular RF settings, some of which resulted in excess beam losses. The experimentally observed beam loss shows a counter-intuitive behavior. Namely, the case (Case-II) with the most significant mismatch oscillation involves less significant beam loss than the modestly mismatched case (Case-I). We have been concerned that the irregular RF setting could induce an unusual beam behavior in the longitudinal phase space to which the counter-intuitive beam loss behavior is attributable, and it has motivated us to conduct a particle simulation to reproduce the experimental result. The simulation indicates that we could have an excess beam loss with an irregular RF setting but it is caused by a simple scraping of the transverse beam edge. This picture leads us to conclude that the beam loss could be caused by satellite particles presumably consisting of protons. Although we need to conduct further studies to confirm this view on the cause of the beam loss, we believe that the particle simulation has provided us with an important insight into the loss mechanism in an actual operation of J-PARC linac.

REFERENCES

- [1] K. Hasegawa, "Recovery of the J-PARC Linac from the Earthquake", to be published in LINAC'12.
- [2] M. Ikegami et.al., "Beam Start-up of J-PARC Linac after the Tohoku Earthquake", IPAC'12, New Orleans, May 2012, THPPC010, p. 3293 (2012).
- [3] M. Ikegami et.al., "Beam Commissioning of J-PARC Linac after Tohoku Earthquake and Its Beam Loss Mitigation", to be published in Procs. 9th Annual Meeting PASJ (Particle Accelerator Society of Japan).
- [4] M. Ikegami et.al., "Beam Loss Mitigation in J-PARC Linac after the Tohoku Earthquake", to be published in LINAC'12.
- [5] Y. Yamazaki ed., "Technical Design Report of J-PARC", KEK Report 2002-13 (2003).
- [6] T. Ito, K. Hirano, private communication.
- [7] T. Ito, K. Hirano, K. Nammo, "Multipactor at SDDL Cavity in J-PARC Linac", to be published in Procs. 9th Annual Meeting PASJ (in Japanese).
- [8] G. Shen, M. Ikegami, Nucl. Instrum. Meth. Phys. Res. A 598 (2009) 361.
- [9] S. Lee et.al., "The Beam Loss Monitor System of the J-PARC Linac, 3 GeV RCS, and 50 GeV MR", EPAC'04, Lucerne, July 2004, THPLT074, p. 2667 (2004).
- [10] H. Sako, M. Ikegami, IEEE Trans. Nucl. Sci., 57 (2010), 57.
- [11] J. Qiang, R.D. Ryne, S. Habib, V. Decyk, J. Comput. Phys., 163 (2001), 434.
- [12] K. R. Crandall et.al., RFQ Design Codes, LA-UR-96-1836.
- [13] Y. Kondo et.al., "Particle Distributions at the Exit of the J-PARC RFQ", LINAC'04, Lübeck, August 2004, MOP19, p. 78.